Interaction of Unsaturated Fatty Acids with the Red Blood Cell Ca^{2+}-ATPase. Studies with a Novel Photoactivatable Probe†

Juan P. F. C. Rossi, José M. Delfino, Ariel J. Caride,‡ and Horacio N. Fernández*

Instituto de Química y Fisicoquímica Biológicas (UBA-CONICET), Facultad de Farmacia y Bioquímica, Junín 956, 1113 Buenos Aires, Argentina

Received June 27, 1994; Revised Manuscript Received November 10, 1994⊗

ABSTRACT: Unsaturated fatty acids, such as oleic acid, increase both the affinity for Ca^{2+} and the maximum effect of the Ca^{2+}-ATPase of red blood cells [Niggli et al. (1981) *J. Biol. Chem. 256,* 8588−8592]. With the aim of examining the structural and kinetic details of the interaction between unsaturated fatty acids and the enzyme, we designed and synthesized 8-(5′-azido-*O*-hexanoylsalicylamido)octanoic acid (AS86), a photoactivatable analogue of unsaturated fatty acids. AS86, interacting noncovalently with the enzyme, shares with oleic acid the following properties: (i) it binds reversibly to the plasma membrane Ca^{2+}-ATPase; (ii) in the absence of calmodulin, AS86 shows a biphasic behavior; i.e., at low concentrations it increases the affinity for Ca^{2+} and the maximum velocity of the enzyme, while at higher concentrations it decreases the maximum velocity; (iii) in the presence of calmodulin, AS86 increases slightly the affinity for Ca^{2+} and decreases the maximum velocity of the Ca^{2+} pump; and (iv) AS86 inhibits the activity of the enzyme devoid of its calmodulin-binding domain after proteolysis. When the reagent is covalently bound to the native enzyme, and then activated by calmodulin, increasing amounts of AS86 decrease the maximum velocity along a hyperbolic curve without modifying the apparent affinity for Ca^{2+}. These results could be explained by the eventual existence of two different kind of sites recognizing the reagent: one influencing the affinity for Ca^{2+} and the other inhibitory of the calmodulin effects. When covalently bound, AS86 exerts its inhibitory effects upon the enzyme lacking the calmodulin-binding domain, thus reflecting that this action is promoted by interaction with a site lying outside this region. The purified enzyme is susceptible to be tagged with ^{125}I-AS86. Both the inhibitory effect on the calmodulin-dependent enzymic activity after covalent binding of AS86 and the photoadduct formation between the enzyme and ^{125}I-AS86 are impaired by the presence of oleic acid in a concentration-dependent fashion. Recognition of photoreactive fatty acid analogues by the purified enzyme could be useful to provide further insight on the location of the interacting sites.

Sarkadi et al. (1982) presented evidence indicating that phospholipase A_2 digestion products, namely, lysophosphatidylcholine and oleic acid, increase the rate of calcium pump activity in calmodulin-depleted inside-out vesicles from red blood cells. A similar effect of unsaturated fatty acids and acidic phospholipids upon the purified enzyme was reported by Niggli et al. (1981b). However, Davis et al. (1987), at variance with the earlier results, found an inhibitory response for oleic acid and the absence of any effect for other unsaturated fatty acids, including linolenic and arachidonic acids. These observations are particularly significant in connection with the widespread occurrence of agonist-stimulated phosphatidylcholine breakdown, associated with activation of phospholipase A_2 and release of unsaturated fatty acids (Exton, 1990).

On the basis of the response to acidic phospholipids of Ca^{2+} pump fragments resulting from limited trypsin proteolysis, Enyedi et al. (1987) and Zvaritch et al. (1990) proposed a discrete protein site for the interaction. This hypothesis has a precedent in protein kinase C, which can be synergically activated by fatty acids and diacylglycerol (El Touny et al., 1990), this protein−lipid interaction presumably occurring through specific sites integrated by Zn structural motifs (Bell & Burns, 1991).

With the aim of further characterizing the nature of the modulation exerted by unsaturated fatty acids on the Ca^{2+} pump, we synthesized and tested 8-(5′-azido-*O*-hexanoylsalicylamido)octanoic acid (AS86),[1] a novel photoreactive probe susceptible to be tagged with ^{125}I, with a conformation resembling that of oleic acid.

EXPERIMENTAL PROCEDURES

Reagents. 5-Aminosalicylic acid, *N*-hydroxysuccinimide, sodium azide, 8-aminooctanoic acid, chloramine-T, calmodulin−agarose, ATP, Mops, and enzymes were purchased from Sigma Chemical Co.; hexanoic anhydride was obtained from Fluka; silica gel 60 Å (40−63 μm) was from Aldrich Chemical Co.; oleic acid was from Analabs; and Na^{125}I (15−17 Ci/mg) was from New England Nuclear. All other chemicals and solvents were of analytical grade quality. Tetrahydrofuran and pyridine were dried over 4 Å molecular sieves; toluene was treated with P_2O_5 and distilled. Solutions

† This work was supported by grants from Universidad de Buenos Aires, Fundación Antorchas, and CONICET.

‡ Present address: Department of Biochemistry and Molecular Biology, Mayo Clinic Foundation, Rochester, MN 55905.

⊗ Abstract published in *Advance ACS Abstracts,* March 1, 1995.

[1] Abbreviations: Bicine, *N,N*-bis(2-hydroxyethyl)glycine; Mops, 3-(*N*-morpholino)propanesulfonic acid; S86, 8-(*O*-hexanoylsalicylamido)octanoic acid; AS86, 8-(5′-azido-*O*-hexanoylsalicylamido)octanoic acid; ^{125}I-AS86, 8-(3′-[^{125}I]iodo-5′-azido-*O*-hexanoylsalicylamido)octanoic acid; SUV, small unilamellar vesicles.

0006-2960/95/0434-3802$09.00/0

were prepared in glass double distilled water. Recently drawn human blood for the isolation of Ca^{2+}-ATPase was obtained from the Hematology Section of the Hospital de Clínicas General San Martín (Argentina).

Measurements. Nuclear magnetic resonance spectra (NMR) were recorded on a Varian FT-80A spectrometer at 80 MHz, and the chemical shifts were referenced to the TMS resonance. Electronic impact ionization mass spectrometry was carried out on a Shimadzu GCMS QP-1000 operated in the EI mode at an ionization voltage of 70 eV, and fast atom bombardment mass spectrometry was performed by Dr. Stuart L. Schreiber at the Chemistry Department, Harvard University. UV spectrophotometry was carried out on a Jasco UVIS 7850, and densitometric quantitation of autoradiograms, on a Shimadzu CS-930.

Protein concentration was determined according to the method of Lowry et al. (1951), as modified by Peterson (1977).

Ionic Ca^{2+} concentration in the incubation medium was measured using a selective Ca^{2+} electrode, as described by Kratje et al. (1983).

Synthesis of 8-(5′-Azidosalicylamido)octanoic Acid. 5-Azidosalicylic acid was obtained as described previously (Atlasovich et al., 1993). The subsequent coupling reaction was similar to that used by Kinnunen et al. (1990). Typically, solid *N*-hydroxysuccinimide (2.2 mmol) and dicyclohexylcarbodiimide (2.2 mmol) were incorporated to a cooled solution of 5-azidosalicylic acid (2.0 mmol) in tetrahydrofuran (4 mL), and the mixture was stirred overnight at 4 °C. The solution was then filtered, pyridine (4.4 mmol) and 8-aminooctanoic acid (2.2 mmol) were added, and the mixture was stirred for another 72 h. At the end, the reaction mixture was filtered, acidified by the addition of 12 M HCl (370 μL), and dried under vacuum. The solid residue, dissolved in ethyl acetate (20 mL), was extracted with 0.01 M HCl. The organic phase was then dried over Na_2SO_4, filtered, and dried under vacuum. The product was not purified further, but residual humidity was thoroughly eliminated by repeated additions of dry toluene followed by vacuum drying. The material recovered (337 mg, 53% yield) consisted of a single photoreactive compound (R_f = 0.41), slightly contaminated with two non-photoreactive substances, as judged by TLC on silica gel plates developed in chloroform/methanol (10:1 v/v). Analysis by EI mass spectrometry of a sample of this product showed the parent molecular ion at *m/e* = 321 ($M + H^+$) and major signals at *m/e* = 292 ($M^+ - N_2$) and 275 ($M^+ - N_2 - OH$). ^{1}H-NMR ($CDCl_3$, 80 MHz): δ 1.22 (m, 10 H), 2.18 (m, 2 H), 3.27 (m, 2 H), 6.28 (s broad, 1 H), 6.94 (m, 3 H aromatic). A minor contamination was evidenced by a multiplet at δ 2.64.

Synthesis of 8-(O-Hexanoyl-5′-azidosalicylamido)octanoic Acid. Acylation of 300 mg of 8-(5′-azidosalicylamido)-octanoic acid (approximately 0.94 mmol) was carried out by mixing with 1.22 mmol of hexanoic acid, 1.22 mmol of pyridine, and 2.44 mmol of hexanoic anhydride, and stirring overnight at room temperature. The mixture, which turned clear as the reaction progressed, was resolved in a silica gel column eluted with dichloromethane/methanol (20:1 v/v) and the product recovered by eliminating the solvent under a nitrogen stream. Residual methanol was thoroughly eliminated by successive additions of dichloromethane followed by vacuum drying. The oily residue turned crystalline after standing at 4 °C for 3 weeks in an evacuated desiccator over molecular sieves. The product yielded a single spot (R_f = 0.52) on TLC plates eluted with chloroform/methanol (10:1 v/v), which turned yellow after UV irradiation. FAB mass spectrometry showed the expected parent ion at *m/e* = 417 $(M - H)^-$ and prominent peaks at *m/e* = 389 $(M - N_2 - H)^-$, 319 $(M -$ hexanoyl$)^-$, and 291 $(M - N_2 -$ hexanoyl$)^-$. ^{1}H-NMR ($CDCl_3$, 80 MHz): δ 0.75 (t, 3 H), 1.27−1.47 (m, 16 H), 2.17 (m, 2 H), 2.40 (m, 2 H), 3.18−3.27 (m, 2 H), 6.24 (s broad, 1 H), 7.02−7.35 (complex, 3 H aromatic).

Synthesis of 8-(3′-[^{125}I]Iodo-5′-azidosalicylamido)octanoic Acid and 8-(O-Hexanoyl-3′-[^{125}I]iodo-5′-azidosalicylamido)-octanoic Acid. 8-(5′-Azidosalicylamido)octanoic acid (3.2 μg; 10 nmol) added as a 10 mM ethanol solution, was dried in the bottom of a 3 × 40 mm tube, and 10 μL of 0.3 M sodium phosphate buffer, pH 7.4, 0.5 mCi of $Na^{125}I$, and 2.5 μL of 1 mM chloramine-T were successively added. After stirring, the reaction was allowed to proceed for 5 min. The mixture was then brought to pH 2.5 by the addition of 2 μL of 1.5 M HCl, 2 μL of dimethylformamide was added, and the product was recovered by extraction with 30 μL of benzene. The radioiodinated compound (specific activity: 24 Ci/mmol) was purified by TLC using chloroform/methanol (10:1 v/v) as the solvent. The predominant radioactive spot (R_f = 0.37), which accounted for 89% of the total radioactivity present, was eluted with absolute ethanol and kept at −25 °C until use. Acylation of 8-(3′-[^{125}I]iodo-5′-azidosalicylamido)octanoic acid was performed just preceding a labeling experiment. A typical procedure was as follows: a sample was dried in a 0.1 mL V-vial, 0.5 μL of an equimolar mixture of pyridine, hexanoic acid, and hexanoic anhydride was added, and the tube was flushed with N_2 and let stand overnight at room temperature. Excess reagent was eliminated by adding 5 μL of dry toluene and vacuum drying for 6 consecutive times. An autoradiography of a TLC analysis of the product showed a predominant spot with a mobility similar to that of unlabeled AS86.

Conformational Search of Compounds. All modeling and molecular mechanics calculations were performed on a DEC Micro Vax 2000 with the package MacroModel v.3.0 and Batchmin v.2.6 (W. C. Still, Columbia University: Mohamadi et al., 1990) which uses N. Allinger's 1985 MM2 force field parameter set with additions.

Preparation of Isolated Red Cell Membranes. Fresh blood from hematologically normal adults collected on acid/citrate/dextrose solutions was routinely used. Red cell membranes were prepared following the procedure of Gietzen et al. (1981) with some modifications, as follows: 1 volume of red cells (washed 3 times with 150 mM NaCl) was lysed in 8 volumes of lysing solution (1 mM EGTA, 15 mM Tris-HCl, pH 7.4) at 4 °C. Membranes were spun down at 17000*g* during 20 min and then washed twice with lysing solution. The membranes were then suspended in 8 volumes of lysing solution, incubated 15 min at 37 °C in this solution, and spun down at 17000*g* during 20 min. This step was repeated once. Membranes were then washed with 8 volumes of 15 mM Tris-HCl (pH 7.4), resuspended in 1 volume of the same solution, and stored at −20 °C. This procedure yields membranes devoid of endogenous calmodulin. Calmodulin was purified from bovine brain as described by Kakiuchi et al. (1981).

For treatment with trypsin, the membranes were washed and suspended in media containing 120 mM KCl, 30 mM

Tris-HCl (pH 7.4 at 37 °C), 0.5 mM EGTA, and 10 μg/mL trypsin (60 units/mg). The mixture was incubated at 4 °C, and after 4 min trypsin action was terminated by the addition of soybean trypsin inhibitor (final concentration: 200 μg/mL). Then, membranes were spun down and resuspended in 50 mM Bicine-K (pH 8.3 at 25 °C). The size of the Ca^{2+}-ATPase digestion products was checked by [^{32}P] phosphorylation, SDS−PAGE, and visualization of the [^{32}P] intermediates by autoradiography (Rossi et al., 1988). Enzymic activity was about 80% of the initial and was insensitive to calmodulin.

Purification of the Ca^{2+}-ATPase from Human Erythrocytes. Blood samples were drawn and immediately mixed with an anticoagulant solution containing 1 mM EDTA-Tris (pH 7.4 at 37 °C) and 150 mM NaCl. Afterward, red cells were washed 3 times with 10 volumes of cold 150 mM NaCl. Calmodulin-depleted erythrocyte membranes were prepared using a hypotonic solution according to the procedure described above. The membrane suspension was frozen at −20 °C. Ca^{2+}-ATPase was isolated by the calmodulin affinity chromatography procedure described by Roufogalis and Villalobo (1989). Purified enzyme was stored in 0.05% *n*-dodecyl decaethylene glycol monoether, 0.1% asolectin, 20 mM Mops-KOH (pH 7.4 at 4 °C), 2 mM EDTA, 2 mM $CaCl_2$, 2 mM DTT, and 300 mM KCl in liquid nitrogen until use.

Ca^{2+}-ATPase Activity. ATPase activity was measured at 37 °C in a medium containing 120 mM KCl, 30 mM Tris-HCl (pH 7.4 at 37 °C), 4 mM $MgCl_2$, 1 mM EGTA, 2 mM ATP, and $CaCl_2$ (enough to reach the Ca^{2+}_{free} concentration indicated on the figures). Ca^{2+}-ATPase activity was taken as the difference between the activity measured in the above medium and that measured in the same medium without calcium. The protein concentration ranged between 50 and 100 μg/mL (membrane assay) or 2 and 5 μg/mL (purified enzyme assay). The release of P_i from the nucleotide was estimated according to the procedure of Fiske and Subbarow (1925).

Assay of the Oleic Acid and AS86 Effect upon Ca^{2+}-ATPase Activity. Oleic acid and AS86 were incorporated into membranes (1 mg of protein/mL) suspended in 0.02 M Mops and 0.3 M KCl, by adding the compounds dissolved in ethanol/propylene glycol (1:3 v/v, 1% final ethanol concentration) while vigorously stirring. In some cases, membranes containing AS86 were irradiated in Falcon Petri dishes at 254 nm and at 3 cm from the lamp during 5 min. The reagent not covalently bound was eliminated by incubating the membrane suspension for 20 min with 3 volumes of a phosphatidylcholine liposome preparation: SUVs, 4.5 mg of egg phosphatidylcholine/mL, prepared in 130 mM KCl, 3.7 mM $MgCl_2$, and 20 mM Tris-HCl (pH 7.4 at 37 °C), by sonication at room temperature for 20 min. The suspension was then diluted 10-fold with water, and the membranes were recovered by centrifugation at 15000*g* for 10 min. This procedure was repeated once. The Ca^{2+}-ATPase activity was measured as indicated above.

The purified enzyme (30−60 μg/mL) was incubated with AS86 incorporated as described above. In experiments involving cross-linking, the enzyme was diluted with 10 volumes of a 4.5 mg/mL egg phosphatidylcholine SUV suspension before measuring the Ca^{2+}-ATPase activity.

Covalent Linking of Radioiodinated Probes to Purified Ca^{2+}-ATPase and SDS−PAGE Analysis. The radioactive reagent, alone or with the addition of oleic acid, was redissolved by adding 0.5 μL of ethanol followed by 1.5 μL of propylene glycol, and with vigorous stirring, 50 μL (3.2 μg) of the purified Ca^{2+}-ATPase suspension was added. After 10 min at room temperature the sample was irradiated, through the mouth of the vial, with a Desaga UVIS at 3 cm from the lamp at 254 nm during 5 min ([^{125}I-AS86 and 11-(*O*-acetyl-3′-[^{125}I]iodo-5′-azidosalicylamido)undecanoic acid) or at 366 nm during 2 min (8-(3′-[^{125}I]iodo-5′-azidosalicylamido)octanoic acid). An equal volume of Laemmli sample buffer was added next, and the mixture was let stand overnight at room temperature prior to SDS−PAGE (6.3% T, 4.8% C, 0.2% SDS) according to Laemmli (1970). Radioactive material in the dried gels was visualized by autoradiography on Kodak XAR-5 film aided by Lightning Plus intensifying screens at −70 °C for 1−10 days. In some cases, radioactivity associated with the bands was quantified by densitometric analysis of the autoradiograms.

Analysis of the Data. All measurements were performed in duplicate or triplicate. Except where indicated, experiments presented in Results were chosen as representative of at least 2 independent experiments. The equations were fitted to the experimental data by a nonlinear regression procedure based on the Gauss−Newton algorithm (Fraser & Suzuki, 1973; Rossi & Garrahan, 1989). The dependent variable was assumed to be homoscedastic (constant variance) and the independent variable to have negligible error. The "best fitting equation" was considered as that which gave the minimal standard deviation of the regression and the least biased fit. Parameters were expressed as mean value ± standard error.

RESULTS

General Design of the Photoprobe AS86. AS86 (top right structure in Figure 1) was designed to resemble unsaturated fatty acids. *Ortho* substitution of the aliphatic branches at the arylazido group in the former was intended to mimic the double bond present in the latter. The azido function is positioned outwardly at the convex face of the molecule, thus improving the chance of productive reaction of the photogenerated nitrene with neighboring molecules. Unlike other reagents of this class (Waggoner & Bernlohr, 1990; Kinnunen et al., 1990), the phenol group *para* with respect to the azido orients the substitution of ^{125}I *meta* with respect to the photoreactive group, thus minimizing steric hindrance in the reaction of the nitrene.

The route of synthesis, described in the Experimental Procedures, should allow investigators to vary the overall length of the molecule and the position of the kink at the aromatic nucleus, by choosing an appropriate combination of fatty acid and ω-amino fatty acid as starting materials, thus giving rise to a family of compounds of this general type.

Conformational Search of S86. We undertook molecular mechanics calculations to evaluate the extent of similarity between AS86 and natural unsaturated fatty acids, such as oleic acid. For the purpose of this analysis, we chose S86 as the model compound for AS86, since the azido group was not adequately parametrized in the MM2 force field used. However, preliminary calculations, after inclusion of experimental bond lengths and angles for the azido group (Scriven, 1984) into the MM2 force field, showed that

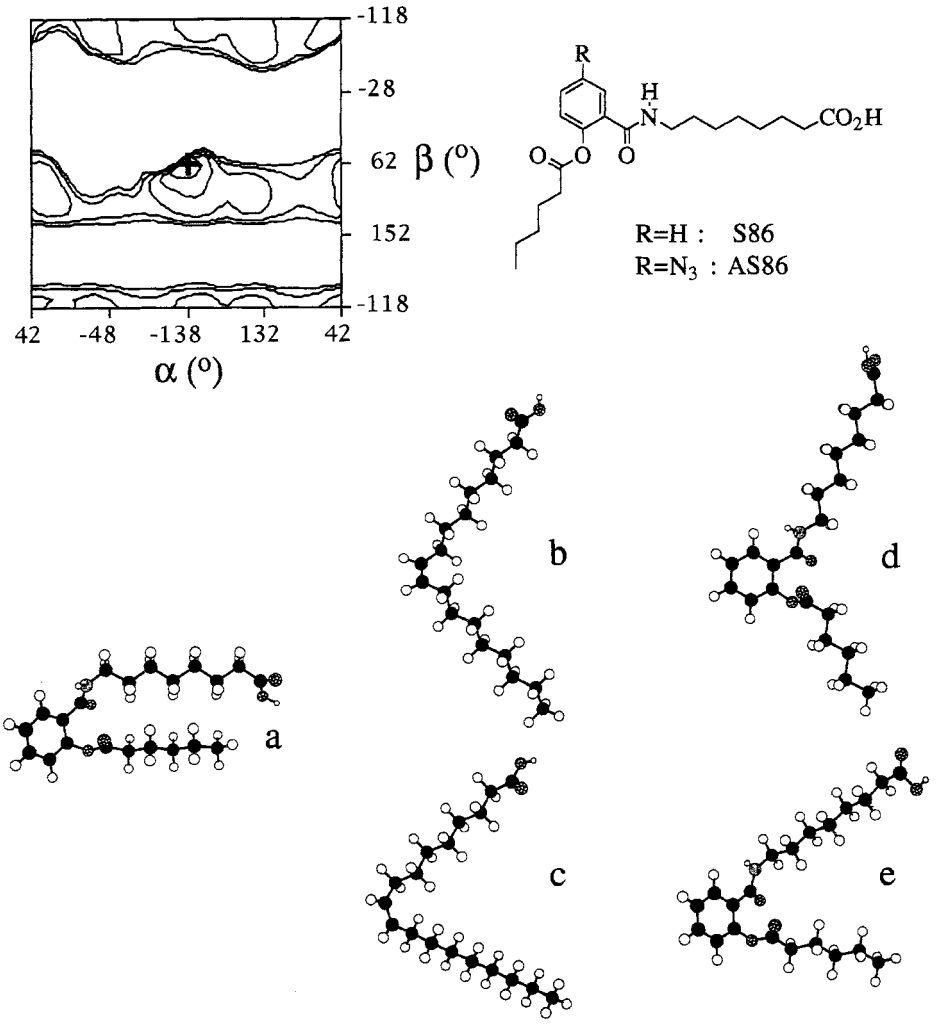

FIGURE 1: Top: Energy level map (left) around torsion angles α and β of S86 (right). Energy values were calculated for conformer **1** of S86 (Table 1, structure *a* below) on a grid of 36 by 36 points (i.e., 10° resolution) employing the ENERGY MAP submode of MacroModel v.3.0 (W. C. Still, Columbia University: Mohamadi et al., 1990) with the MM2 force field. Five contour isoenergy levels are plotted, and the cross indicates the position of the global minimum. Bottom: Superimposition of S86 and oleic acid structures. Global minimum conformers of S86 (**1**, Table 1; structure *a*) and oleic acid (**1** and **2**, Table 1; structures *b* and *c*). Structures *d* and *e* result from least-squares flexible superimposition (allowing free rotation of torsional angles C−NH and OC−C) of conformer *a* over oleic acid conformers *b* and *c*, respectively. After the initial fit, each rotamer of conformer *a* was subjected to 1000 minimization cycles using the block diagonal Newton−Raphson algorithm to eliminate local tensions around the rotated dihedral angles. 17 atomic pairs along the chains were used for each comparison. The residual RMS deviations between *b* and *d* and between *c* and *e* were 0.805 and 0.878 Å, respectively.

minimized structures of S86 and AS86 are almost superimposable (results not shown). This is not unexpected given the distal position of the azido substituent.

The aliphatic chains of the starting model of S86 were constructed in their fully extended (least energy) forms and the amide linkage torsion was set to *trans* (180°). Modeling of the S86 structure indicates that the overall conformation of the molecule is critically determined by the two dihedral angles connecting the substituents to the phenyl ring, namely, α: C−Ph and β: O−Ph. Torsions around the phenyl ring substituents in S86 and around the double bond in oleic acid were explored by a full-space grid search method (INPUT MULTIC submode of MacroModel). Twenty and thirteen starting structures for S86 and oleic acid, respectively, were generated by systematically rotating α and β at 60° torsional resolution, followed by elimination of high energy conformers (>20 kJ/mol). These structures were individually minimized *in vacuo* with Batchmin, following the block diagonal Newton−Raphson method, until convergence was reached (residual gradient ≈ 0.03 kJ/(mol·Å)). Duplicate structures (identical and enantiomeric structures) were then discarded, and all unique minima within a 20 kJ/mol window above the global minimum (conformer **1**) were recorded (Table 1). A test for imaginary vibrational modes was computed for each minimized structure to verify that they correspond to true minima.

Examination of the conformational space around α and β of conformer **1** of S86 was achieved with the ENERGY MAP submode (top left diagram of Figure 1), which allows a 360° rotation of each aliphatic branch as a rigid body. The α,β pair of dihedral angles in conformer **1** of S86 lies at the absolute energy minimum (indicated by a cross at the center of the diagram). In addition, each one of the other dihedral angles in conformer **1** of S86 was shown to lie at or near the bottom of the well corresponding to its absolute minimum.

Similar calculations carried out on an analogue of S86 devoid of aliphatic chains, i.e., 2-acetoxy-*N*-methylbenzamide, indicated a global minimum for a conformer with α = −152.1° and β = 66.8°, close to conformer **1** of S86. In

Table 1: Minimum Energy Conformations of S86 and Oleic Acid

conformer	α^a (deg)	β^a (deg)	energy^b (kJ/mol)
S86			
1	−139.1	62.5	−32.0
2	−25.5	−108.7	−24.9
3	−53.2	91.7	−24.6
4	150.8	−65.1	−18.4
5	55.3	−88.8	−16.6
6	−159.5	−120.8	−16.6
oleic acid			
1	−96.2	−97.1	−15.6
2	−84.4	115.3	−15.3
3	−121.6	−162.8	−11.7

[a] For S86, α and β are the dihedral angles C−Ph and O−Ph, respectively. For oleic acid, α and β are the dihedral angles C_8-C_9 and $C_{10}-C_{11}$, respectively. [b] Energy values according to the MM2 force field, as implemented in Batchmin v.2.6 (W. C. Still, Columbia University: Mohamadi et al., 1990).

addition, the energy map of this molecule is very similar to that of S86 (results not shown).

An independent conformational search of S86, carried out with Batchmin and employing an optimized Monte Carlo method (Chang et al., 1989) starting from a planar *all-trans* construction, yielded 63 fully minimized conformers (residual gradient ≈ 0.03 kJ/(mol·Å)) after 317 Monte Carlo cycles. For this calculation, apart from varying α and β, additional relaxation of structures was allowed by freeing torsions around dihedral angles C−CNH, C−NH, O−CO, and OC−C, while mantaining the amide linkage fixed at 180° and the planarity of the phenyl ring. The distribution of lowest energy conformers clusters around four distinct (nonenantiomeric) regions in the conformational space defined by α and β. A remarkably good agreement with results obtained with the grid search was achieved, since all these regions were sampled by the conformers bearing α−β torsions similar to those described in Table 1. Those structures within 6 kJ/mol above the global minimum (α = 142.4°, β = −66.4°, energy = −36 kJ/mol) are represented mainly by conformers **1**, **2**, and **4**. Structures ranging between −30 and −22 kJ/mol are sampled mainly by conformer **2** and less frequently by conformers **1** and **3**. Finally, the energy range between −22 and −16 kJ/mol is populated by all six conformers in Table 1, and predominantly by conformers **1**, **4**, and **6**.

The global minimum structure of S86 (**1**, Table 1; Figure 1, structure *a*) was compared to the two very close in energy minimum structures obtained with oleic acid (**1** and **2**, Table 1; Figure 1, structures *b* and *c*). At first, clear differences are apparent between the "U" shape of the former and the "V" shape of the latter. However, after allowing free rotation around torsional angles C−NH and OC−C in S86 during superimposition and further relaxation of the structures by further minimization, a close fit between the molecules could be demonstrated (residual RMS deviations lower than 0.88 Å).

Effect of Noncovalently Bound AS86 on the Ca^{2+}-ATPase Activity. Figure 2A shows that in the absence of calmodulin, as the concentration of AS86 is increased in red cell membranes, the Ca^{2+}-ATPase activity rises, passes through a maximum, and then drops tending to a constant value, which is about 2-fold the activity in the absence of AS86. On the other hand, in the presence of calmodulin and at concentrations of AS86 up to 200 μM, the enzymic activity increases slightly before decreasing toward the basal (no-calmodulin) values as it was estimated by nonlinear regression. At concentrations higher than 2500 μM (not shown), AS86 causes a further inhibition of Ca^{2+}-ATPase activity both in the absence and in the presence of calmodulin.

A similar biphasic effect on the Ca^{2+}-ATPase activity of isolated red cell membranes was also found by using oleic acid (Figure 2B), albeit at a somewhat lower range of concentrations (by a factor of 5) than those assayed for AS86. Our results on the effect of oleic acid on Ca^{2+}-ATPase activity were similar to those reported before for inside-out vesicles by Sarkadi et al. (1982). It seems, therefore, that noncovalently bound AS86 reproduces well the effects of oleic acid on the enzymic activity.

Removal of Noncovalently Bound AS86 from Red Cell Membranes. Table 2 shows the effect of extensive washing with a phosphatidylcholine suspension (SUVs) of isolated membranes previously incubated with 360 μM of AS86. Before the cleansing of membranes, Ca^{2+}-ATPase activity increased as a consequence of the presence of AS86, 5.7 times in the absence of calmodulin, and about 10% in the presence of 120 nM of this modulator. By contrast, after thorough washing of membranes with phosphatidylcholine liposomes, a negligible effect on Ca^{2+}-ATPase was observed for both basal and calmodulin-stimulated activities as compared to the original control values. This result suggests that the reagent was almost completely eliminated from membranes by the phosphatidylcholine suspension. Parallel experiments showed that this procedure was also effective to remove oleic acid from red cell membranes.

The apparent discrepancy between the activation level elicited by AS86 in this experiment and those shown in Figure 2 could be accounted for by the influence of the Ca^{2+} concentration upon the activity of the enzyme, as will be shown below.

Inactivation of Ca^{2+}-ATPase in the Presence of AS86 by Irradiation. Figure 3 shows an experiment designed to test the effects of AS86 on the Ca^{2+}-ATPase activity by irradiation of a red blood cell membrane suspension containing 360 μM of the reagent. Figure 3A shows the absorbance spectra of the species recovered from membranes containing AS86 after irradiation. Upon photolysis, the absorbance at 251 nm, a band related to the azido group of AS86, decreases exponentially with a $t_{0.5}$ of 63.2 ± 19.3 s (inset). Results in Figure 3B show that, in the presence of calmodulin, the Ca^{2+}-ATPase activity also decreases as a function of time according to an exponential curve, approaching a constant value. The best fit rendered a $t_{0.5}$ equal to 83.3 ± 4.5 s. Conversely, in the absence of calmodulin, only a slight decrease in the Ca^{2+}-ATPase activity was observed. Enzymic activity of controls without AS86 showed no significant differences after 10 min of irradiation.

The $t_{0.5}$ of both inactivation of Ca^{2+}-ATPase and the photoinduced decay of AS86 were comparable, suggesting that photolysis of AS86 and photoreaction of Ca^{2+}-ATPase with AS86 are cause-related phenomena.

On the other hand, after 5 min of irradiation of membranes containing AS86, a spectrophotometric estimate indicated that 95.7% of the AS86-derived species was removed by washing the samples with phosphatidylcholine liposomes, 2.8% was recovered with the lipidic fraction of the membranes after extraction with ethanol, and 1.5% was found associated with the protein fraction dissolved by SDS.

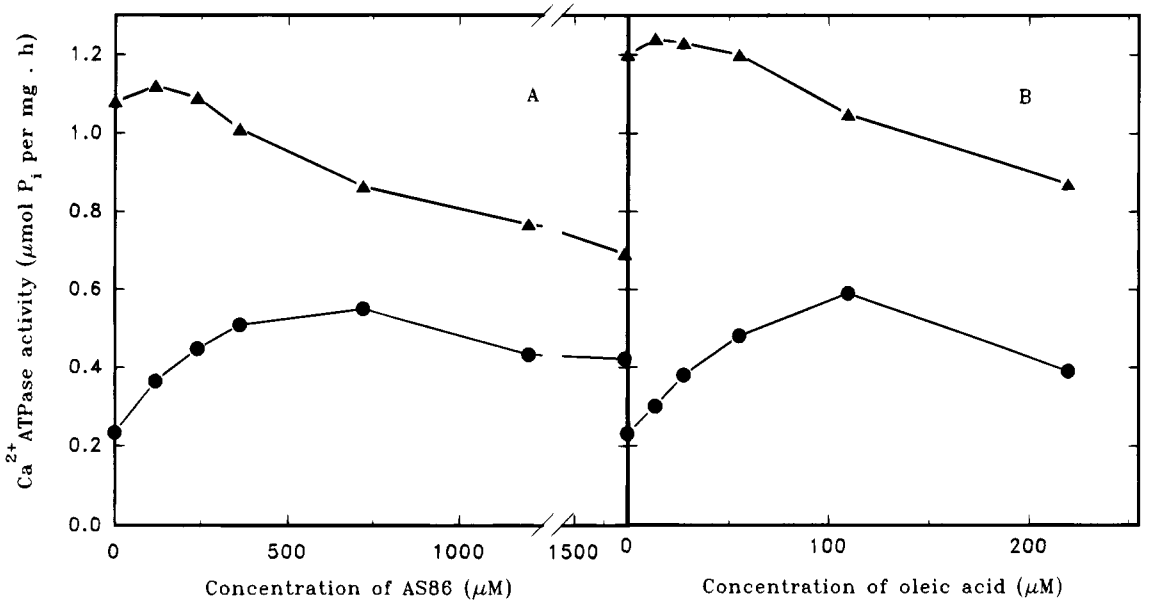

FIGURE 2: Effect of noncovalently bound AS86 (A) and oleic acid (B) on Ca^{2+}-ATPase activity. AS86 or oleic acid was added to isolated membranes as described in the Experimental Procedures. Ca^{2+}-ATPase activity was measured in media with 0 nM (●) and 120 nM (▲) calmodulin. The concentration of Ca^{2+} was 3 μM. Each point is the mean of four independent experiments.

Table 2: Removal of AS86 from Red Blood Cell Membranes[a]

addition	Ca^{2+}-ATPase activity (μmol of P_i/(mg of protein·h)) basal	120 nM calmodulin
none	0.28 ± 0.01	1.82 ± 0.05
360 μM AS86	1.60 ± 0.04	2.00 ± 0.06
360 μM AS86 followed by washing	0.32 ± 0.02	1.85 ± 0.05

[a] Membranes were incubated with or without the reagent during 20 min at room temperature and, then, were washed with a suspension of phosphatidylcholine liposomes (SUVs) as described in the Experimental Procedures. The indicated Ca^{2+}-ATPase activity, measured in a medium containing 10 μM Ca^{2+}, is the mean ± SD of three independent experiments.

Figure 4 shows the effect of exposure to UV radiation of red blood cell membranes containing AS86 on the Ca^{2+}-ATPase activity as a function of increasing concentrations of the reagent. In the absence of calmodulin, the enzymic activity was not affected up to 240 μM AS86, but the calmodulin-dependent activity decreased along a hyperbolic curve approaching the basal activity. At concentrations of AS86 higher than 240 μM, an additional inhibition of both calmodulin and basal activities was also detected. It seems, therefore, that the covalent binding of AS86 to the enzyme predominantly abrogates the response of Ca^{2+}-ATPase to calmodulin.

Oleic acid (175−1400 μM), coincubated with AS86 (480 μM) and Ca^{2+}-ATPase, was able to effectively prevent the inhibition of the calmodulin-dependent enzymic activity caused by the photoreaction of AS86 (Figure 5), pointing to the fact that this photoprobe not only mimics the effect of oleic acid, but also competes with it for the binding sites in the enzyme. The protective effect of oleic acid is most evident at the low concentration range (175−350 μM), close to the range at which oleic acid exerts a sensible effect on the enzymic activity (50−220 μM, Figure 2B).

Effect of AS86 on the Kinetic Parameters of the Ca^{2+}-ATPase. The effects of AS86 on the apparent affinity for Ca^{2+} (K_{Ca}) and on the maximum velocity of the Ca^{2+}-ATPase (V_{max}) are shown in Table 3. Noncovalently bound AS86 decreases K_{Ca} and increases V_{max} with respect to control values. This effect is most evident in the absence of calmodulin, although in the presence of this modulator, a small but significant decrease in K_{Ca} was also seen. No further increase in V_{max} occurs in the presence of calmodulin.

These results suggest that AS86 interacts noncovalently with a site(s) which modulates the affinity for Ca^{2+} of the pump, since the maximum velocity was reached at lower Ca^{2+} concentrations. Such interaction does not seem susceptible to becoming covalently stabilized, taking into account that the modification undergone by the protein, following irradiation in the presence of AS86, does not modify the apparent affinity for Ca^{2+} of the Ca^{2+}-ATPase, both in the presence and in the absence of calmodulin. On the other hand, the covalently stabilized interaction would not produce large changes in the maximum activity of the enzyme under basal conditions, but significantly abrogates the activation induced by calmodulin.

Control samples irradiated in the absence of AS86 (not shown) did not evidence any deleterious effects on the activity of the enzyme.

Effect of AS86 on the Partially Proteolyzed Enzyme. It is well-known that controlled proteolysis with trypsin of the Ca^{2+}-ATPase leads to fragmentation of the protein into a number of products, some of which retain ATPase activity (Rossi & Schatzmann, 1982; Zvaritch et al., 1990). In order to assess whether AS86 binds to the calmodulin-binding domain of the Ca^{2+}-ATPase, we tested the effects of AS86 on the enzyme fragment devoid of this domain, with a molecular mass of 80 kDa. Ca^{2+}-ATPase activity measured in isolated membranes subjected to tryptic proteolysis showed a negligible response to calmodulin. Figure 6A shows that noncovalently bound AS86 inhibits the activity of proteolyzed Ca^{2+}-ATPase along a hyperbolic curve that levels off to a constant value. No further activation by AS86 could be detected, above the maximum value measured for the proteolyzed enzyme. On the other hand, Figure 6B shows

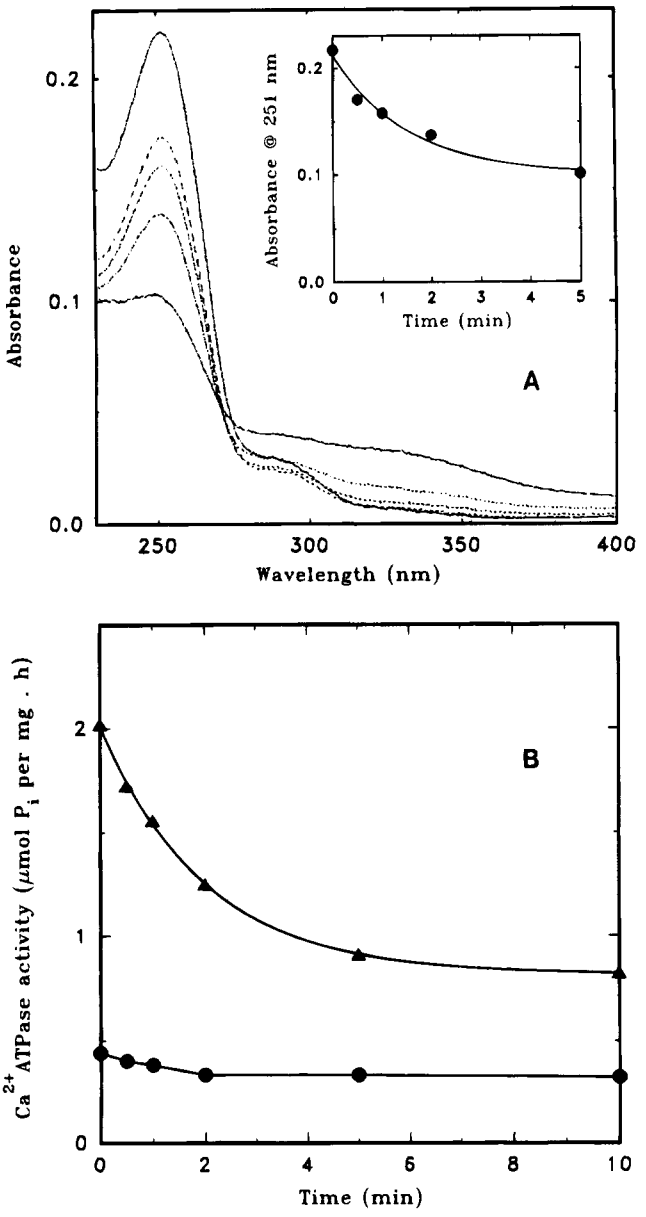

FIGURE 3: Comparison between time courses of photolysis of AS86 and of inactivation of Ca^{2+}-ATPase. Red blood cell membranes, mixed with 360 μM AS86, were irradiated for the indicated times, and then excess reagent was eliminated as described in the Experimental Procedures. (A) Aliquots of the supernatants from the first centrifugation were dissolved in ethanol to record the UV spectra. The absorbance at 251 nm as a function of time was adjusted by the equation:

$$v = A_1 e^{-kt} + A_2 \quad (1)$$

where A_1 is the difference between the absorbance values at 251 nm at $t = 0$ and $t = t_\infty$; A_2 is the absorbance at t_∞; and k is the apparent rate constant for the decay in absorbance, with $A_1 = 0.11 \pm 0.01$, $A_2 = 0.10 \pm 0.01$, and $k = 0.65 \pm 0.19$ min^{-1}. (B) The Ca^{2+}-ATPase activity was measured in the absence (●) and in the presence of 120 nM calmodulin (▲). The Ca^{2+} concentration was 10 μM. The following equation was adjusted to the experimental points:

$$v = P_1 e^{-kt} + P_2 \quad (2)$$

where P_1 is the Ca^{2+}-ATPase activity inhibitable by AS86; P_2 is the remnant Ca^{2+}-ATPase activity; and k is the apparent rate constant for inhibition, with $P_1 = 1.20 \pm 0.02$ μmol of P_i/(mg of protein·h), $P_2 = 0.81 \pm 0.01$ μmol of P_i/(mg of protein·h), and $k = 0.50 \pm 0.02$ min^{-1}.

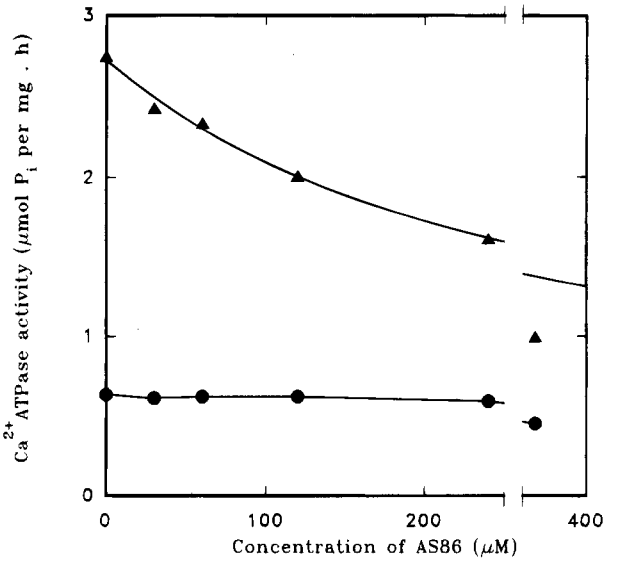

FIGURE 4: Effect of covalently bound AS86 on Ca^{2+}-ATPase activity. The enzymic activity in red cell membranes is plotted as a function of the concentration of added AS86, after irradiation and washing with phosphatidylcholine SUVs, in the absence (●) and in the presence (▲) of 120 nM calmodulin. Ca^{2+} concentration was 10 μM. The following equation was adjusted to the experimental data in the presence of calmodulin:

$$v = V_m K_i/(K_i + [AS86]) + V_{rem} \quad (3)$$

where V_m is the Ca^{2+}-ATPase activity inhibitable by AS86; V_{rem} is the noninhibitable Ca^{2+}-ATPase activity; and K_i is the apparent inhibition constant, with $V_m = 2.41 \pm 0.60$ μmol of P_i/(mg of protein·h), $V_{rem} = 0.32 \pm 0.10$ μmol of P_i/(mg of protein·h), and $K_i = 280 \pm 90$ μM.

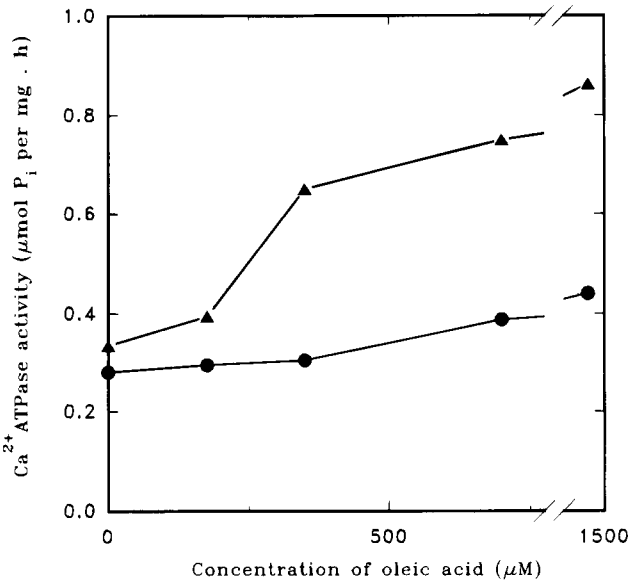

FIGURE 5: Protective action of oleic acid on the effect of covalently bound AS86 on Ca^{2+}-ATPase activity. The enzymic activity in red cell membranes is plotted as a function of the concentration of added oleic acid in a mixture with 480 μM AS86, after irradiation and washing with phosphatidylcholine SUVs. Enzymic activity was measured in a medium containing 3 μM Ca^{2+}, in the absence (●) and in the presence (▲) of 120 nM calmodulin.

the effect of covalently bound AS86. Similarly to noncovalently bound AS86, Ca^{2+}-ATPase activity drops hyperbolically after irradiation in the presence of increasing concentrations of the reagent. Furthermore, covalent binding results in a greater inhibition of the enzyme: the K_i for inhibition

Table 3: Effect of AS86 on the Kinetic Parameters of the Ca^{2+}-ATPase[a]

procedure	K_{Ca} (μM)	V_{max} (μmol of P_i/(mg of protein·h))
controls		
basal	15.60 ± 1.70	1.05 ± 0.02
calmodulin	3.80 ± 0.27	3.05 ± 0.05
AS86, nonirradiated		
basal	1.26 ± 0.25	1.92 ± 0.12
calmodulin	1.86 ± 0.20	2.88 ± 0.13
AS86, irradiated		
basal	14.25 ± 1.48	0.65 ± 0.09
calmodulin	2.80 ± 0.15	0.98 ± 0.05

[a] Enzymic activity was assayed as a function of increasing concentrations of Ca^{2+}. The values for half-maximum activation (K_{Ca}) and the maximum velocity (V_{max}) were estimated by the following equation to the experimental data:

$$v = V_{max}/(1 + K_{Ca}/[Ca^{2+}])^n \quad (4)$$

The value of n in the equation was 1 in the absence and 2 in the presence of calmodulin (see Rossi and Rega (1989) for an explanation). Calmodulin and AS86 concentrations were 120 nM and 360 μM, respectively. Results are expressed as the mean ± SD of three independent experiments.

was 174 ± 28 μM for the nonirradiated versus 35.9 ± 6.1 μM for the photolyzed preparations.

Effect of AS86 on the Purified Ca^{2+}-ATPase. Similarly to the effects already described on isolated red blood cell membranes, in the absence of calmodulin, noncovalently bound AS86 produces a biphasic response on the activity of purified Ca^{2+}-ATPase: the activity increases up to 90 μM AS86 and then hyperbolically decreases (Figure 7A). In the presence of calmodulin, the activity remains constant up to approximately 40 μM AS86, followed by a sharp decay that runs parallel to the inhibition of the basal activity. These results, in turn, resemble those reported for oleic acid by Niggli et al. (1981b).

On the other hand, covalently bound AS86 (Figure 7B) monotonically inhibits the calmodulin-dependent activity, leaving unaffected the basal activity up to 100 μM. Concentrations of AS86 higher than 100 μM inhibit the calmodulin-independent Ca^{2+}-ATPase activity. It is worth mentioning that these effects were elicited at lower reagent concentrations when acting on the purified enzyme than in isolated membranes (cf. Figures 2 and 4 with Figure 7A,B, respectively).

It seems, therefore, that noncovalent or covalent interactions of AS86 with purified Ca^{2+}-ATPase are similar to those of the enzyme located in its natural milieu in the erythrocyte membrane.

Cross-Linking of Radioiodinated Fatty Acid Photoprobes with Purified Ca^{2+}-ATPase. Another line of evidence demonstrating the interaction of the reagent with Ca^{2+}-ATPase came from the direct visualization of the covalent species generated after irradiation. Figure 8A shows an autoradiogram of the complexes formed by irradiation of a preparation of the purified enzyme and ^{125}I-AS86, subjected to SDS−PAGE (lane 2). The radioactive species gave rise to a single band of molecular mass estimated at 138 kDa. For comparison purposes, cross-linking with a different fatty acid analogue, 11-(*O*-acetyl-3′-[^{125}I]iodo-5′-azidosalicylamido)undecanoic acid (Atlasovich et al., 1993), was also examined (lane 3). Experiments testing the latter probe (not shown) evidenced no effect on the Ca^{2+}-ATPase activity before or after photoactivation over a wide range of concentrations. In keeping with this behavior, the reagent labeled poorly the purified enzyme. The truncated precursor of ^{125}I-AS86, 8-(3′-[^{125}I]iodo-5′-azidosalicylamido)octanoic acid, was also found less efficient than radioiodinated AS86 to establish covalent links with the enzyme (lane 1). Oleic acid was shown to effectively compete with ^{125}I-AS86 for the binding to the Ca^{2+}-ATPase: Figure 8B shows an autoradiographic analysis after SDS−PAGE of the photoadducts generated after irradiation of the purified enzyme incubated with ^{125}I-AS86 and increasing amounts of oleic acid. At high concentration (600 μM), oleic acid essentially eliminates the formation of any covalent complex between the enzyme and ^{125}I-AS86 (lane 8), whereas the largest difference in the relative yield of the radioiodinated covalent complexes is observed at low concentration (25 μM, lane 5). This compares very well with the covalent inactivation of the Ca^{2+}-ATPase by AS86 (Figure 7B), where the largest decrease of the calmodulin-dependent enzymic activity is also evidenced at low concentrations of the ligand (25−75 μM AS86).

DISCUSSION

It was described that unsaturated fatty acids, like oleic acid, and acidic phospholipids, like phosphatidylserine and phosphatidylinositol, increase both the affinity for Ca^{2+} and the maximum effect of the Ca^{2+}-ATPase of red blood cells devoid of endogenous calmodulin (Ronner et al., 1977; Niggli et al., 1981a; Sarkadi et al., 1982). It was also proposed that, similarly to calmodulin and partial proteolysis by trypsin, those activating agents seem to act directly on the enzyme and not via membrane modifications (Niggli et al., 1981b). Conversely, other authors postulated that the effect of phospholipids and fatty acids could occur as a consequence of modification of the lipid bilayer and not directly on the enzyme (Nelson & Hanahan, 1985).

With the purpose of examining the structural and kinetic details of the interaction between the enzyme and unsaturated fatty acids, we have synthesized the photoactivatable probe AS86. AS86 possesses a negative charge and a shape intended to mimic the bend of the double bond, which could represent essential features of the fatty acids to interact with the Ca^{2+} pump. Inspection of the conformational ensemble of S86 (Table 1 and Figure 1) shows that the energetically most favored conformers (**1**, **2**, and **3**) adopt a "U" shape, followed by two more open "V"-shaped forms (**4** and **5**) and a somewhat more extended form (**6**). Similarly, the lowest energy conformers of oleic acid (**1** and **2**) adopt "V" shapes, while conformer **3** is rather more extended. Discrimination of the individual energy components to the overall energy of conformers **1**−**3** of S86 indicates a significant contribution of favorable van der Waals interactions, between 10 and 20 kJ/mol less than for conformers **4**−**6**. Interestingly, closer examination of conformers **1**−**3** shows an almost perfect interdigitation of aliphatic hydrogens along the two branches of the molecule, giving rise to parallel "U"-shaped close-packed structures. Nevertheless, interactions at the hinge region, whose shape is defined by the pair α,β of dihedral angles, predominate, as suggested by the closeness of these values for conformer **1** to those corresponding to the global minimum conformer of an analogue of S86 devoid of aliphatic chains (2-acetoxy-*N*-methylbenzamide).

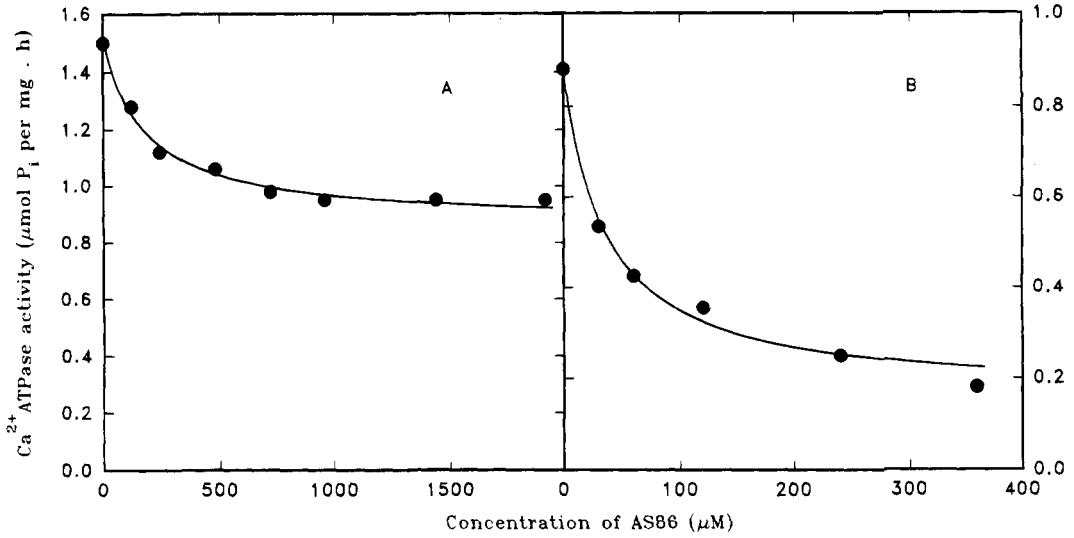

FIGURE 6: Effect of (A) noncovalently bound and (B) covalently bound AS86 on the Ca^{2+}-ATPase activity of partially proteolyzed enzyme. See Figures 2 and 4 and the Experimental Procedures for details. The concentration of Ca^{2+} was 3 μM. Equation 3 was adjusted to the experimental data, with (A) $V_m = 0.654 \pm 0.027$ μmol of P_i/(mg of protein·h), $V_{rem} = 0.868 \pm 0.023$ μmol of P_i/(mg of protein·h), and $K_i = 174 \pm 28$ μM; and (B) $V_m = 0.718 \pm 0.034$ μmol of P_i/(mg of protein·h), $V_{rem} = 0.159 \pm 0.027$ μmol of P_i/(mg of protein·h), and $K_i = 35.9 \pm 6.1$ μM. Plotted values represent the results of two independent experiments.

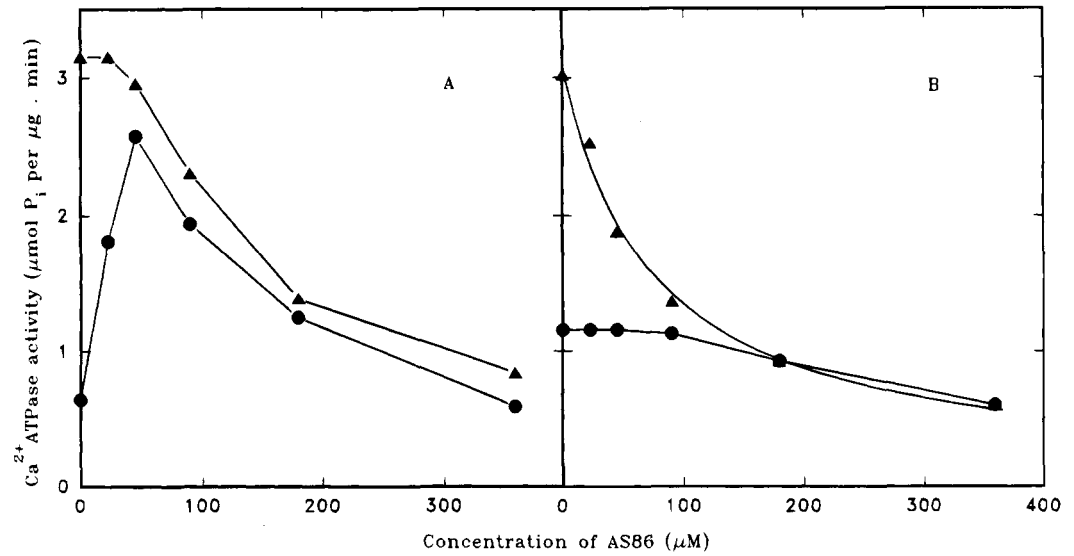

FIGURE 7: Effect of AS86 on the purified Ca^{2+}-ATPase. (A) Ca^{2+}-ATPase activity as a function of the concentration of noncovalently bound AS86, in the absence (●) and in the presence (▲) of 120 nM calmodulin. (B) Ca^{2+}-ATPase activity as a function of the concentration of added AS86, after photoactivation and washing with phosphatidylcholine SUVs, in the absence (●) and in the presence (▲) of 120 nM calmodulin. The concentration of Ca^{2+} was 10 μM.

Consistently, rotamers of conformer **1** of S86 resembling oleic acid and originated by torsions around C−NH and OC−C (Figure 1) show somewhat higher overall energies (−17.8 and −21.1 kJ/mol for structures *d* and *e*, as compared to −32.0 kJ/mol for conformer **1**, structure *a*), contributed mainly by the unstacking of the aliphatic chains, as indicated by the correspondingly higher value of the van der Waals component (55.9 and 56.3 kJ/mol for structures *d* and *e*, as compared to 36.3 kJ/mol for conformer **1**, structure *a*). This favorable stacking interaction, although evidently a major energetic contribution determining the most likely structure predicted *in vacuo*, may not be so relevant in the membrane milieu where this fatty acid analogue is bound to dwell. Here, intermolecular van der Waals contacts with other aliphatic chains from phospholipids may energetically compensate for the loss of intramolecular stacking interactions and give rise to significant population of open conformers, more similar in shape to those of unsaturated fatty acids. Therefore, it seems safe to conclude that the design of the hinge region provides a constraint to the flexibility of this molecule which bears close resemblance with the effect of the double bond present in natural unsaturated fatty acids.

Results in this paper show that AS86 interacts reversibly with the plasmic membrane Ca^{2+} pump. In this condition, AS86 reproduces the biphasic behavior of oleic acid on Ca^{2+}-ATPase activity; i.e., in the absence of calmodulin, as the concentration of AS86 rises, the activity first increases, then passes through a maximum, and finally tends to the level observed in the absence of the reagent. It was observed before that unsaturated fatty acids and acidic phospholipids produce inhibition of the Ca^{2+} pump at concentrations close to the activating ones (Niggli et al., 1981a,b; Sarkadi et al., 1982; Missiaen et al., 1989), thus masking further activation of the enzyme. In this connection, Davis et al. (1987) failed

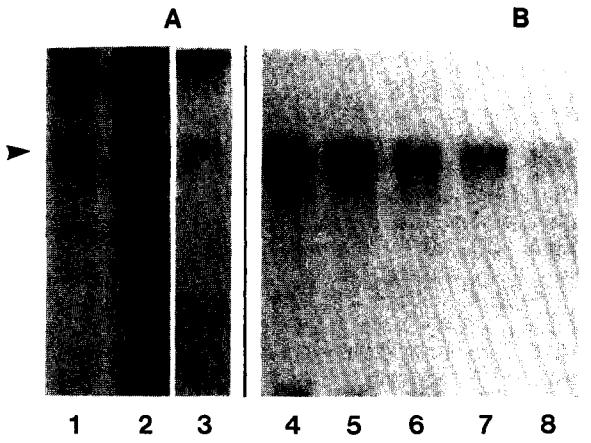

FIGURE 8: (A) Autoradiogram of 0.46 μM purified Ca^{2+}-ATPase (12 pmol) incubated with either 0.54 μM 8-(3′-[^{125}I]iodo-5′-azidosalicylamido)octanoic acid (24 Ci/mmol, 14 pmol, 0.33 μCi) (lane 1), 0.54 μM ^{125}I-AS86 (24 Ci/mmol, 14 pmol, 0.33 μCi) (lane 2), or 0.46 μM 11-(*O*-acetyl-3′-[^{125}I]iodo-5′-azidosalicylamido)-undecanoic acid (28 Ci/mmol, 12 pmol, 0.33 μCi) (lane 3), irradiated as indicated in the Experimental Procedures, and subjected to SDS−PAGE. (B) Autoradiogram of 0.46 μM purified Ca^{2+}-ATPase (12 pmol) incubated with 1.6 μM ^{125}I-AS86 (35 Ci/mmol, 40 pmol, 1.4 μCi) and oleic acid (the relative densities of the main bands are shown in parentheses): 0 μM (1.0, lane 4), 25 μM (0.53, lane 5), 75 μM (0.37, lane 6), 225 μM (0.25, lane 7), and 600 μM (0.09, lane 8), irradiated as indicated in the Experimental Procedures and subjected to SDS−PAGE. In all cases, the samples applied to gels contained 25 μL of the incubation mixture. The arrow indicates the position of the enzyme (138 kDa).

to reproduce the stimulatory effects of oleic acid on the Ca^{2+}-ATPase from isolated red blood cell membranes. The biphasic activation−inhibition behavior induced by AS86 was also seen in the presence of calmodulin, although the activation of the enzyme was less apparent since, at the concentrations of Ca^{2+} used to measure the activity, the enzyme was nearly maximally activated by calmodulin (Figures 2A and 7A).

By contrast, covalent binding of AS86 to the enzyme primarily prevents the activation of Ca^{2+}-ATPase by calmodulin, leaving untouched the basal activity up to 240 μM AS86 (Figure 4). Such an effect was elicited by AS86 concentrations lower than those required when acting by noncovalent interaction (Figure 2A), thus indicating that covalent binding enhances the inhibitory effect of the reagent. Oleic acid exerts a protective effect on the inhibition triggered by covalent binding of AS86 (Figure 5), most likely, by competing with the photoprobe for binding sites responsible for these modulatory effects in the enzyme.

With regard to the effects on the kinetic parameters of the enzyme (Table 3), the noncovalent addition of AS86 to membranes increases both the apparent affinity for Ca^{2+} and the maximum velocity of the Ca^{2+}-ATPase, when assayed in the absence of calmodulin. In the presence of calmodulin, a small increase in the apparent affinity for Ca^{2+} was also noticeable. These results agree well with the observations of Sarkadi et al. (1982) for the effects of lysophosphatidylcholine on Ca^{2+} transport. On the other hand, covalent binding of AS86 does not modify the apparent affinity for Ca^{2+}, both in the absence and in the presence of calmodulin. Under such conditions, the main effect of AS86 was to decrease by more than 3-fold the maximum velocity of the calmodulin-dependent activity. Conversely, in the absence of calmodulin a 38% inhibition was observed, which in turn might not be significant, since at AS86 concentrations higher than 240 μM a small decrease in activity occurs (see Figure 4).

A possible interpretation for the results of Table 3 and Figures 2A and 4 could consist in the eventual existence of two different kinds of sites recognizing AS86: one related to the activation of Ca^{2+}-ATPase, whose occupation by AS86 increases the apparent affinity for Ca^{2+}, and the other which may be responsible for the decrease in the maximum velocity of the enzyme observed in the presence of calmodulin.

Furthermore, the monomodal decay of the enzymic activity as a function of the amount of covalently bound AS86, as shown in Figures 4 and 6B, could suggest that under these conditions only one kind of sites in the Ca^{2+} pump is modified. Taking into account that the covalent link would presumably stabilize a preexisting interaction, it does not appear likely that such a link could alter the modality of the response. However, with the evidence presently available, it is not possible to rule out that the geometric constraints imposed by the covalent link could favor a particular conformation of the sites exclusively associated with an inhibitory effect.

It could be argued that the effects observed for the enzyme irradiated in the presence of AS86 could be due, at least partially, to the covalent binding of the reagent to the membrane phospholipids which constitute the Ca^{2+} pump environment. However, after photolysis and washing with phosphatidylcholine SUVs, spectrophotometric estimates of the reacted probe indicate that almost all of the original amount of AS86 in the sample was recovered in the vesicles, leaving only a negligible amount remaining in the lipids of the membrane (2.8%). This result deems unlikely the possibility that a significant amount of cross-linked products with the membrane phospholipids could remain in the sample to exert any effect on the enzyme. Furthermore, an indirect effect mediated by lipid−AS86 complexes becomes less likely since, in the presence of detergent and at a different lipid:protein ratio, such as that prevailing in experiments performed with purified Ca^{2+}-ATPase (Figure 7), essentially similar results were obtained. On the other hand, direct evidence for the ^{125}I-AS86−enzyme interaction and its covalent stabilization was provided by the visualization of the radioiodinated complexes after SDS−PAGE and autoradiography (Figure 8). In a fashion similar to experiments described above on the covalent inhibition of the Ca^{2+} pump triggered by AS86 (Figure 5), oleic acid acts as a competing ligand, impairing the cross-linking between ^{125}I-AS86 and the enzyme (Figure 8B), further suggesting a direct cause−effect relationship between the covalent binding of the probe to the protein and the inhibition of enzymic activity.

Recently, Filoteo et al. (1992), by using synthetic peptides, demonstrated that acidic phospholipids interact both with peptide G25—a putative binding site in the so-called G region—and with the primary domain for calmodulin (C region). It could be tempting to propose that the chiefly inhibitory effect exerted by AS86 upon the enzyme activated by calmodulin—an effect also observed for acidic phospholipids (Niggli et al., 1981b)—could be due to competition between the probe and calmodulin for the interaction with the C region. Under this hypothesis, the covalent link that AS86 could establish with this site would render the enzyme insensitive to calmodulin. However, the results obtained after cleavage of the enzyme (Figure 6) rule out this hy-

pothesis. Removal of the calmodulin-binding domain by controlled proteolysis with trypsin generated a functional 80 kDa fragment of the enzyme. This fragmentation of Ca^{2+}-ATPase, which leads to full expression of the activity, did not prevent either the noncovalent or the covalent interactions with AS86, since under both conditions Ca^{2+}-ATPase activity was inhibited by the reagent.

Although with the present data it is not possible to give further precision about where AS86 binds to the Ca^{2+} pump, it seems safe to infer the existence of a site(s) outside the C domain able to interact and establish a covalent link with the probe. Peptide G25, which shows a propensity to form an amphiphilic helix endowed with several positive charges and presumably located near the membrane interface (Zvaritch et al., 1990), could be a plausible candidate. The fact that the purified enzyme is susceptible to be tagged with ^{125}I-AS86 could be useful to provide further insight on the location of the interaction sites.

ACKNOWLEDGMENT

We are greatly indebted to Dr. Stuart L. Schreiber from the Chemistry Department, Harvard University, for the mass spectrometry analyses and to Ms. Alejandra Vardaro for her excellent technical assistance.

REFERENCES

Atlasovich, F., Santomé, J. A., & Fernández, H. N. (1993) *Mol. Cell. Biochem. 120*, 15−23.

Bell, R. M., & Burns, D. J. (1991) *J. Biol. Chem. 266*, 4661−4664.

Chang, G., Guida, W. C., & Still, W. C. (1989) *J. Am. Chem. Soc. 111*, 4379−4386.

Davis, F. B., Davis, P. J., Blas, S. D., & Schoenl, M. (1987) *Biochem. J. 248*, 511−516.

El Touny, S., Khan, W., & Hannun, Y. (1990) *J. Biol. Chem. 265*, 16437−16443.

Enyedi, A., Flura, M., Sarkadi, B., Gárdos, G., & Carafoli, E. (1987) *J. Biol. Chem. 262*, 6425−6430.

Exton, J. H. (1990) *J. Biol. Chem. 265*, 1−4.

Filoteo, A. G., Enyedi, A., & Penniston, J. T. (1992) *J. Biol. Chem. 267*, 11800−11805.

Fiske, C. H., & Subbarow, Y. (1925) *J. Biol. Chem. 66*, 375−400.

Fraser, R. D. B., & Suzuki, E. (1973) in *Physical Principles and Techniques of Protein Chemistry* (Leach, S. J., Ed.) Part C, pp 301−355, Academic Press, New York.

Gietzen, K., Wüthrich, A., & Bader, H. (1981) *Biochem. Biophys. Res. Commun. 101*, 418−425.

Kakiuchi, S., Sobue, K., Yamazaki, R., Kambayashi, J., Sakon, M., & Kosaki, G. (1981) *FEBS Lett. 126*, 203−207.

Kinnunen, P. M., Klopf, F. H., Bastiani, C. A., Gelfman, C. M., & Lange, L. G. (1990) *Biochemistry 29*, 1648−1654.

Kratje, R. B., Garrahan, P. J., & Rega, A. F. (1983) *Biochim. Biophys. Acta 731*, 40−46.

Laemmli, U.K. (1970) *Nature 227*, 680−685.

Lowry, O. H., Rosebrough, W. J., Farr, A. L., & Randall, R. J. (1951) *J. Biol. Chem. 193*, 265−275.

Missiaen, L., Raeymaekers, L., Wuytack, F., Vrolix, M., De Smedt, H., & Casteels, R. (1989) *Biochem. J. 263*, 687−694.

Mohamadi, F., Richards, N. G. J., Guida, W. C., Liskamp, R., Lipton, M., Caufield, C., Chang, G., Hendrickson, T., & Still, W. C. (1990) *J. Comput. Chem. 11*, 440−467.

Nelson, D. R., & Hanahan, D. J. (1985) *Arch. Biochem. Biophys. 236*, 720−730.

Niggli, V., Adunyah, E. S., Penniston, J. T., & Carafoli, E. (1981a) *J. Biol. Chem. 256*, 395−401.

Niggli, V., Adunyah, E. S., & Carafoli, E. (1981b) *J. Biol. Chem. 256*, 8588−8592.

Peterson, G. L. (1977) *Anal. Biochem. 83*, 346−356.

Ronner, P., Gazzotti, P., & Carafoli, E. (1977) *Arch. Biochem. Biophys. 179*, 578−583.

Rossi, J. P. F. C., & Schatzmann, H. J. (1982) *Cell Calcium 3*, 583−590.

Rossi, J. P. F. C., & Rega, A. F. (1989) *Biochim. Biophys. Acta 996*, 153−159.

Rossi, J. P. F. C., Gronda, C. M., Fernández, H. N., & Gagliardino, J. J. (1988) *Biochim. Biophys. Acta 943*, 175−182.

Rossi, R. C., & Garrahan, P. J. (1989) *Biochim. Biophys. Acta 981*, 85−94.

Roufogalis, B. D., & Villalobo, A. (1989) in *The Red Cell Membrane, A model for solute transport* (Raess, B. U., & Tunnicliff, G., Eds.) pp 76−83, Humana Press, Clifton.

Sarkadi, B., Enyedi, A., Nyers, A., & Gárdos, G. (1982) in *Transport ATPases* (Carafoli, E., & Scarpa, A., Eds.) pp 329−346, Annals of The New York Academy of Sciences, Vol. 402, New York.

Scriven, E. F. V. (1984) in *Azides and Nitrenes, Reactivity and Utility*, p 96, Academic Press, Orlando.

Waggoner, D. W., & Bernlohr, D. A. (1990) *J. Biol. Chem. 265*, 11417−11420.

Zvaritch, E., James, P., Vorherr, T., Falchetto, R., Modyanov, N., & Carafoli, E. (1990) *Biochemistry 29*, 8070−8076.

BI9414146